Journal of Bone Oncology 32 (2022) 100409

Contents lists available at ScienceDirect

Journal of Bone Oncology

journal homepage: www.elsevier.com/locate/jbo

Research Paper

Protective effect of bisphosphonate on the cortical bone at key locations of the femur in aromatase inhibitor-associated bone loss: A three-dimensional cortical bone mapping study

Namki Hong [a,1], Seung Won Burm [a,1], Graham Treece [b], Jee Ye Kim [c], Min Hwan Kim [d], Seunghyun Lee [a], Sungjae Shin [a], Yumie Rhee [a,*]

[a] Department of Internal Medicine, Severance Hospital, Endocrine Research Institute, Yonsei University College of Medicine, 50-1 Yonsei-ro, Seodaemun-gu, Seoul 03722, South Korea
[b] Department of Engineering, University of Cambridge, Trumpington St, Cambridge CB2 1PZ, UK
[c] Department of Surgery, Severance Hospital, Yonsei University College of Medicine, 50-1 Yonsei-ro, Seodaemun-gu, Seoul 03722, South Korea
[d] Division of Oncology, Department of Internal Medicine, Severance Hospital, Yonsei University College of Medicine, 50-1 Yonsei-ro, Seodaemun-gu, Seoul 03722, South Korea

ARTICLE INFO

Article history:
Received 26 October 2021
Revised 24 December 2021
Accepted 28 December 2021
Available online 29 December 2021

Keywords:
Bisphosphonates
Aromatase inhibitor-associated bone loss
Quantitative computed tomography
Breast cancer
Cortical bone
Proximal femur

ABSTRACT

Aromatase inhibitor treatment in breast cancer is associated with accelerated bone loss and an increased risk of fracture. Bisphosphonates (BPs) are the mainstay treatment of aromatase inhibitor-associated bone loss (AIBL), which might improve femoral bone at key locations prone to fracture. To test this hypothesis, we performed three-dimensional cortical bone mapping based on quantitative computed tomography (QCT) scans in postmenopausal women with early breast cancer who were receiving aromatase inhibitors. Data of subjects who had both baseline and at least one follow-up QCT at Severance Hospital (South Korea) between 2005 and 2015 were analyzed (BP users, n = 93; BP non-users, n = 203). After exclusion of BP users with low medication persistence (proportion of days covered: <50%), BP users and non-users were 1:1 matched (n = 54 for each group) in terms of age, lumbar spine volumetric bone mineral density (LSvBMD), femoral neck areal BMD (FNaBMD), and total hip areal BMD (THaBMD). During a median follow-up of 2.1 years, BP use attenuated bone loss in LSvBMD (+7.2% vs. −3.8%, p < 0.001), FNaBMD (+1.3% vs. −2.7%, p < 0.001), and THaBMD (-0.3% vs. −2.5%, p = 0.024). BP had a protective effect on cortical parameters of femoral bone: estimated cortical thickness (CTh) (+3.3% vs. + 0.1%, p = 0.007) and cortical mass surface density (CMSD, cortical mass per unit surface area was calculated by multiplying cortical BMD with CTh) (+3.4% vs. −0.3%, p < 0.001). CMSD increased by up to 15% at key locations such as the superior part of the femoral neck and greater trochanter. BP prevented the thinning of average CTh of the femoral neck (-1.4% vs. −6.1%, p < 0.001), particularly at the superior anterior quadrant of femoral neck (absolute difference: +12.8% point vs. non-users). Compared to BP non-users, BP users had improved cross-sectional moment of inertia (+4.4% vs. −0.7%, p = 0.001) and less increase in buckling ratio (+1.3% vs. + 7.5%, p < 0.001). In summary, BP use prevented cortical bone deficits observed in AIBL at key locations of the proximal femur.

1. Introduction

Aromatase inhibitors are used as the standard adjuvant therapy for hormone-sensitive breast cancer after mastectomy.[1,2] Aromatase inhibitor induced bone loss (AIBL) in post-menopausal women with early breast cancer is known to be associated with rapid loss of bone density, decrease of trabecular bone score, impaired femoral geometry, and increased incidence of both hip and vertebral fractures.[3-5] In our prior study on patients with AIBL using quantitative computed tomography scans (QCT), we found that aromatase inhibitor use in postmenopausal women was associated with cortical bone thinning, particularly at superior femoral neck lesion.[4]

The cortical bone compartment plays an important role in determining femoral bone strength.[6,7] Cortical thinning at the femoral neck is prevalent in the aged population, and this focal, structural weakness could increase risk of hip fracture.[8,9] Advanced imaging techniques such as cortical bone mapping

* Corresponding author at: Department of Internal Medicine, Endocrine Research Institute, Yonsei University College of Medicine, 50-1 Yonsei-ro, Seodaemun-gu, Seoul 03722, South Korea.
E-mail address: yumie@yuhs.ac (Y. Rhee).
[1] These authors contributed equally to this work.

https://doi.org/10.1016/j.jbo.2021.100409
2212-1374/

(CBM) based on quantitative QCT scans allow measures of cortical bone parameters with the investigation of spatial heterogeneity between study groups.[10-12] CBM was also reported to have potential to improve fracture risk prediction when added to aBMD parameters.[13-15] Given that bisphosphonates (BP) are the mainstay treatment of AIBL, it is important to investigate whether BP use can attenuate cortical bone deficits observed in AIBL at key locations of the proximal femur.[16,17]

In this study, we hypothesized that BP use in AIBL would have a beneficial effect on cortical parameters at key locations of the proximal femur. To test this hypothesis, site-specific longitudinal changes of QCT-derived bone parameters between BP users and non-users, among AI-treated patients, were analyzed using the CBM technique.

2. Materials and methods

2.1. Study subjects

The study flow chart is presented in Fig. 1. Clinical data of patients with early breast cancer who received adjuvant endocrine therapy after breast cancer surgery and underwent a baseline QCT scan between January 2006 and December 2015 at Severance Hospital were retrieved from the Severance Clinical Data Repository System. This study was approved by the institutional review board (IRB) of Severance Hospital (Seoul, Korea), with a waiver for written informed consent for retrospective data review (IRB no. 4–2018-0635). After exclusion of individuals who used tamoxifen or did not have any follow-up QCT data, 354 early breast cancer patients who received aromatase inhibitor treatment during the observation period (between baseline and follow-up QCT scans) were grouped into BP users (n = 148) and non-users (n = 206). Further, BP users with a proportion of days covered by BPs<50% were excluded to ensure drug persistency. Given the older age, lower bone density, and higher serum c-telopeptide level in BP users compared to non-users in the unmatched cohort (Supplementary Table 1), we performed 1:1 propensity score matching based on age at baseline, QCT-derived bone density parameters (including lumbar spine volumetric bone mineral density [LSvBMD], FN areal BMD [FNaBMD], and total hip areal BMD [THaBMD]), and serum c-telopeptide level at baseline to adequately compare BMD changes between baseline and follow-up QCT in BP users and non-users (Supplementary Fig. 1). A total of 108 subjects (54 BP users and 54 non-users) were included in the final analysis. Individuals included in the study had baseline QCT done within 3 months prior to or after the time of initiation of aromatase inhibitors (Supplementary Fig. 2). As we excluded individuals who were on bisphosphonate treatment prior to baseline QCT testing (Fig. 1), all subjects in this study received bisphosphonate treatment at the time of or after baseline QCT testing.

2.2. QCT protocol

Baseline and follow-up QCT scans were performed using a LightSpeed VCT (GE Healthcare, Chicago, IL, USA; n = 87, 81%) or SOMATOM Definition AS+ (Siemens Healthineers, Forchheim, Ger-

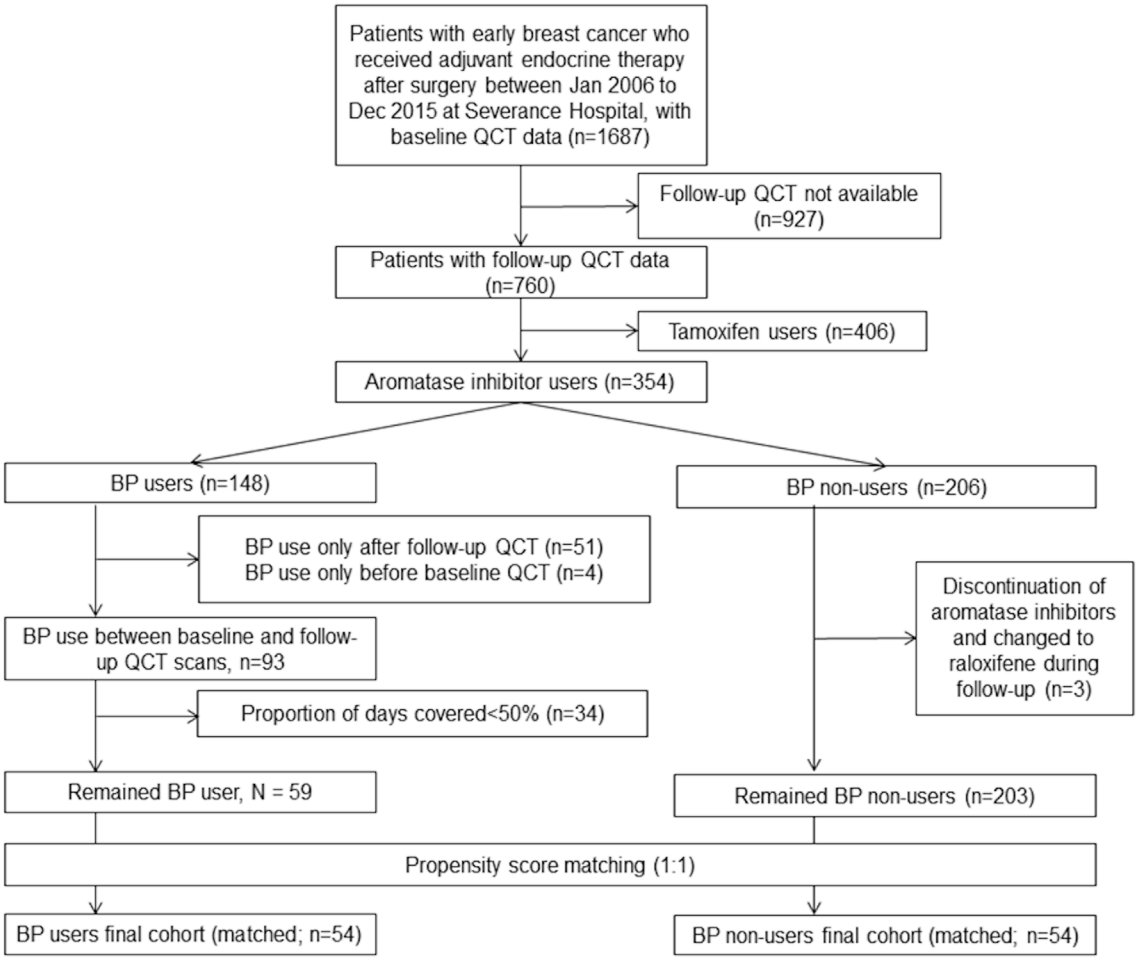

Fig. 1. Study flow. Abbreviations: BP, bisphosphonate; QCT, quantitative computed tomography.

many; n = 21, 19%), with a scan protocol of 120 kVp, 150 mA, and a 50-cm scan field of view. All paired images were taken using the same CT scanners. A liquid dipotassium phosphate intrascan phantom (Model 3; Mindways Software, Inc., Austin, TX, USA) was included in each scan. CT images were reconstructed at a slice thickness of 3 mm for LS and 1 mm for proximal femur using standard body reconstruction kernel, with an in-plane pixel size of 512 × 512 and display field-of-view of 250 mm. QCTPro software (Mindways Software, Inc.) was used to analyze the QCT scans. LSvBMD was calculated as the average vBMD of L1 and L2. Along with vBMD, dual-energy X-ray absorptiometry (DXA)-equivalent aBMD and T-score for the proximal femur was calculated using a CT X-ray absorptiometry program (Mindways Software, Inc.) [18].

2.3. Cortical bone mapping

CBM of the proximal femur was performed according to the previously proposed CBM pipeline, a surface-based technique to reveal the localized skeletal changes and significance from clinically available low-resolution QCT data [11]. Briefly, bone properties including cortical thickness (CTh, mm), cortical BMD (CBMD, mg/cm^3), endocortical trabecular density (ECTD, mg/cm^3), and cortical mass surface density (CMSD, mg/cm^2; cortical mass per unit surface area was calculated by multiplying CBMD with CTh) were calculated at each of roughly 8,000 to 12,000 locations covering the surface of the bone, which was represented as a triangular mesh. To compare the obtained bone properties among multiple subjects and time points, each surface was registered to a template (canonical) hip surface, with individual cortical data transferred to the canonical surface. The mapped individual cortical data were then used to build generalized linear regression models, along with potential regressors such as time points and intervention. Statistical parametric mapping was used to visualize localized regions of the surface with significant difference in time points and intervention. A previous study showed that the coefficient of variation for repeat scanning for individual measurements (at intervals of 3 months) was 6%, 3%, 5%, and 9% for CTh, CBMD, CMSD, and ECTD, respectively [15].

2.4. Femoral neck geometry analysis

The Bone Investigational Toolkit (Mindways Software, Inc.) was used to calculate 3D FN geometry parameters from QCT scans. FN geometry parameters such as cross-sectional area, CTh, cross-sectional moment of inertia (CSMI), section modulus (Z), and buckling ratio (BR) were obtained at FN area, with CTh further analyzed by quadrants (superior anterior, superior posterior, inferior anterior, and inferior posterior) [19]. All CBM and QCT analyses in this study was performed by a single analyst who had>3 years of experience.

2.5. Statistical analysis

The clinical characteristics of study subjects (BP users vs. non-users) were compared using independent two-sample t-tests, Wilcoxon rank sum tests, or chi-square tests, as appropriate. A paired *t*-test was used to compare the changes in bone density between baseline and follow-up QCT scans in BP users and non-users. Propensity score matching was performed using the Stata 'psmatch2' command, with the nearest-neighbor algorithm on a 1:1 basis without replacement. A caliper of 0.2 × standard deviation of log-transformed propensity score was used [20]. Covariate balance was checked using standardized mean difference, with a threshold > 0.2 (20%) indicating substantial imbalance [21]. After propensity score matching, the standardized mean differences decreased to < 0.2 in all matched variables (Supplementary Fig. 1). Percentage changes (%) in bone parameters between BP users and non-users were compared using an independent two sample *t*-test. A linear regression model was built to assess the independent effect of BP use on changes in femoral neck estimated CTh on average and in each quadrant with adjustment for covariates. In statistical parametric mapping, random field theory was used to correct multiple comparisons to control the overall image-wise chance of false positives. Statistical parametric mapping was performed using MATLAB (Release R2019a, The MathWorks, Inc., MA, USA). All statistical analyses were performed using Stata 14.1 (College station, TX, USA). The statistical significance level was set at a two-sided p value of < 0.05.

3. Results

3.1. Characteristics of study subjects

A total of 108 subjects (54 BP users and 54 BP non-users) were analyzed in a propensity score-matched cohort (mean age: 62.4 years). In this matched cohort, BP users and non-users did not differ significantly in terms of age (62.6 vs. 61.6 years), LSvBMD (77.2 vs. 80.7 mg/cm^3), FNaBMD (0.564 vs. 0.576 g/cm^2), or THaBMD (0.676 vs. 0.677 g/cm^2; p > 0.05 for all; Table 1). BP users and non-users had similar prevalence of comorbidities, distribution of cancer-related adjuvant therapies and cancer stages, and laboratory values including calcium, phosphate, and vitamin D level at baseline. Prevalence of prior fracture, glucocorticoid exposure, and rheumatoid arthritis did not differ significantly between two groups. For BP users, the median proportion of observation period covered by BP prescription was 80%, with an interquartile range of 68%–93%. In the BP group, oral risedronate (35 mg weekly or 150 mg monthly) was the most commonly used BP (n = 41, 76%), followed by oral alendronate (70 mg weekly; n = 9, 17%) and oral ibandronate (150 mg monthly; n = 4, 7%).

3.2. Changes in QCT-derived bone density parameters

In the matched cohort, the median follow-up duration between QCT scans was 2 years (760 vs. 757 days in BP users and non-users, respectively; p = 0.327). The volumetric bone densities at the LS (-4.2%), FN (-3.3%), and TH (-4.7%) decreased significantly in BP non-users during aromatase inhibitor treatment, whereas BP use showed a protective effect against the deterioration of bone density caused by aromatase inhibitor use (LS: +5.5%; FN: −0.5%; TH: −1.2%; Table 2). Similar findings were observed for changes in FNaBMD and THaBMD.

3.3. Localized bone changes in CBM

The results of CBM analysis are presented in Fig. 2. BP use had a favorable effect on preserving the average CMSD (+3.4% vs. −0.3%, p < 0.001), CTh (+3.3% vs. + 0.1%, p = 0.007), and ECTD (+1.8% vs. −4.3%, p = 0.004) of the proximal femur. Further, 3D CBM revealed that BP treatment in aromatase inhibitor users had protective effects on specific key locations of the proximal femur, including superior FN and greater trochanter regions, with a prominent effect on CTh at the superior FN. The protective effect of BP on ECTD was significant at the lesser trochanter region (Supplementary Fig. 3).

3.4. Effect of bisphosphonate on changes in bone parameters

BP use was associated with improved volumetric bone density at lumbar spine (+10.9%, p < 0.001) and femoral neck (+2.2%, p = 0.018) after adjustment for covariates (Table 3). Effect of BP use on total hip was prominent in CMSD (+3.7%, p < 0.001) than

Table 1
Characteristics of study subjects.

	Bisphosphonate users (N = 54)	Bisphosphonate non-users (N = 54)	P value
Age, year	62.6 ± 6.9	61.6 ± 8.1	0.516
Body mass index, kg/m^2	24.6 ± 3.0	24.9 ± 3.3	0.526
Diabetes mellitus	12 (22)	12 (22)	0.999
Hypertension	11 (20)	17 (31)	0.188
Adjuvant chemotherapy	31 (57)	30 (55)	0.846
Adjuvant radiotherapy	35 (65)	35 (65)	0.999
Pathologic stage 2–3	22 (41)	22 (41)	0.999
Estimated glomerular filtration rate (ml/min/1.73 m^2)	89 ± 15	88 ± 18	0.783
Serum calcium, mg/dL	9.1 ± 0.5	9.1 ± 0.5	0.999
Inorganic phosphorus, mg/dL	3.9 ± 0.6	3.9 ± 0.7	0.708
25-hydroxyvitamin D, ng/mL	19 ± 9	16 ± 9	0.059
Serum C-telopeptide, ng/mL	0.694 [0.333 to 0.941]	0.686 [0.401 to 0.927]	0.954
Previous fracture, n(%)*	2 (3.7)	0 (0.0)	0.153
Glucocorticoid use, n(%)†	5 (9.3)	6 (11.1)	0.750
Rheumatoid arthritis, n(%)‡	1 (1.8)	1 (1.8)	0.999
LSvBMD, mg/cm^3	77.2 ± 18.4	80.7 ± 24.5	0.390
FNaBMD, g/cm^2	0.564 ± 0.070	0.576 ± 0.075	0.401
FNvBMD, mg/cm^3	261 ± 34	265 ± 33	0.570
THaBMD, g/cm^2	0.676 ± 0.091	0.677 ± 0.091	0.934
THvBMD, mg/cm^3	248 ± 38	249 ± 30	0.913
QCT follow-up duration, days	760 [732–1115]	757 [720–1095]	0.327
Proportion of days covered, %	80 [68–93]	N/A	N/A

Abbreviations: LS, lumbar spine; FN, femoral neck; TH, total hip; vBMD, volumetric bone mineral density; aBMD, areal bone mineral density; N/A, not applicable; QCT, quantitative computed tomography. Proportion of days covered: percentage of duration between baseline and follow-up QCT by bisphosphonate prescription records (drug persistence). To report p value, two-sample independent *t*-test, Wilcoxon rank-sum test, and chi-square test were used as appropriate.
*Presence of diagnosis codes for any major osteoporotic fracture including spine, wrist, hip, and upper arm.
†Any exposure to glucocorticoid during one year prior to baseline QCT date.
‡Presence of Diagnosis codes for rheumatoid arthritis

vBMD (+1.5%, p = 0.120). In FN geometry quadrant analysis, BP use protected against the deterioration in average FN CTh (-1.4% vs. −6.1%) in all quadrants (superior anterior: −7.9% vs. −20.7%; inferior anterior: −1.7% vs. −5.9%; and inferior posterior: +2.6% vs. −0.6%; p < 0.05 for all) except the superior posterior quadrant (-10.4% vs. −18.4%, p = 0.188; Fig. 3). BP use showed favorable effects on changes in CSMI (+4.4% vs. −0.7%, p = 0.001), Z (+1.1% vs. −1.7%, p = 0.013), and BR (+1.3% vs. + 7.5%, p < 0.001) of the FN during aromatase inhibitor use. The effect of BP use on average CTh at FN (+4.7% point difference between BP users and non-users, 95% confidence interval: +2.2 to 7.1, p < 0.001) and the quadrants remained independent after adjustment for age, baseline FN vBMD, and c-telopeptide level (Table 3).

4. Discussion

Our study demonstrates that BP use in postmenopausal women with early breast cancer who were receiving aromatase inhibitor treatment could prevent cortical bone loss at key locations of the proximal femur. BP users had beneficial effects in preserving LSvBMD, THaBMD, and CBM parameters such as CMSD, CTh, and ECTD at the proximal femur when compared to age- and baseline BMD-matched non-users. The protective effect of BP against cortical bone deficit observed in AIBL was most prominent at the superior part of FN and the greater trochanteric region, showing substantial heterogeneity. The association of BP use with volumetric BMD gain at the femoral neck and lumbar spine remained robust after adjustment for age, baseline FNvBMD, and c-telopeptide level.

Several studies have shown favorable effects of BP use on postmenopausal women with early breast cancer on aromatase inhibitor treatment. Patients with AIBL treated with oral risedronate showed BMD changes of + 2.3% at LS and + 0.6% at TH, whereas the placebo group showed −1.7% and −2.7% decreases at 24 months after active treatment [22]. Another study with oral risedronate use in postmenopausal women who were receiving anastrozole treatment showed a + 1.1% gain in BMD at LS and −0.7% loss in BMD at TH after 36 months of follow-up, while those given placebo showed a −2.6% and −3.5% loss in BMD at LS and TH, respectively [23]. In line with previous findings, we observed clear net gain in QCT-derived lumbar spine and femoral neck vBMD up to + 7% by BP use during median two-year follow-up. Furthermore, we investigated geospatial heterogeneity of BP effects on longitudinal changes in cortical parameters at the proximal femur. To our knowledge, our study is the first to use QCT and 3D CBM techniques to assess the positive impact of BP in patients with AIBL, which could support the recent guidelines on BP treatment in postmenopausal women with AIBL [24].

Using the CBM technique, we were able to find substantial geospatial heterogeneity in cortical bone changes by BP use in AIBL. Protective effect of BP against cortical bone deficit in AIBL was noted particularly at the superior femoral neck region. Several studies showed that cortical vBMD loss and cortical bone thinning of proximal femur measured by QCT were important predictors of hip fracture independent of DXA-derived aBMD.[25,26] Of note, in

Table 2
Changes in QCT-derived bone density during aromatase inhibitor use.

	Bisphosphonate users (N = 54)				Bisphosphonate non-users (N = 54)				
	Baseline	Follow-up	Difference	P value*	Baseline	Follow-up	Difference	P value*	P for differences between groups†
LS vBMD, mg/cm^3	77.2 ± 18.4	81.5 ± 17.8	+4.3 ± 11.3	0.006	80.7 ± 24.5	77.4 ± 24.9	−3.3 ± 9.7	0.015	<0.001
FN aBMD, g/cm^2	0.564 ± 0.070	0.570 ± 0.070	+0.006± 0.031	0.157	0.576 ± 0.075	0.557 ± 0.071	−0.016 ± 0.032	<0.001	<0.001
FN T-score	−2.4 ± 0.6	−2.4 ± 0.6	+0.0 ± 0.2	0.180	−2.4 ± 0.6	−2.5 ± 0.6	−0.1 ± 0.2	<0.001	<0.001
FN vBMD, mg/cm^3	261 ± 34	259 ± 35	−2 ± 12	0.145	265 ± 33	256 ± 32	−9 ± 13	<0.001	0.013
TH aBMD, g/cm^2	0.676 ± 0.091	0.673 ± 0.091	−0.003 ± 0.032	0.510	0.677 ± 0.091	0.659 ± 0.086	−0.018 ± 0.038	<0.001	0.024
TH T-score	−2.2 ± 0.7	−2.2 ± 0.7	−0.0 ± 0.3	0.515	−2.2 ± 0.7	−2.3 ± 0.7	−0.1 ± 0.3	<0.001	0.024
TH vBMD, mg/cm^3	248 ± 38	245 ± 36	−3 ± 12	0.040	249 ± 30	242 ± 28	−7 ± 13	<0.001	0.126

Abbreviations: LS, lumbar spine; FN, femoral neck; TH, total hip; vBMD, volumetric bone mineral density; aBMD, areal bone mineral density.
*Two sample paired *t*-test. †Two sample independent *t*-test.

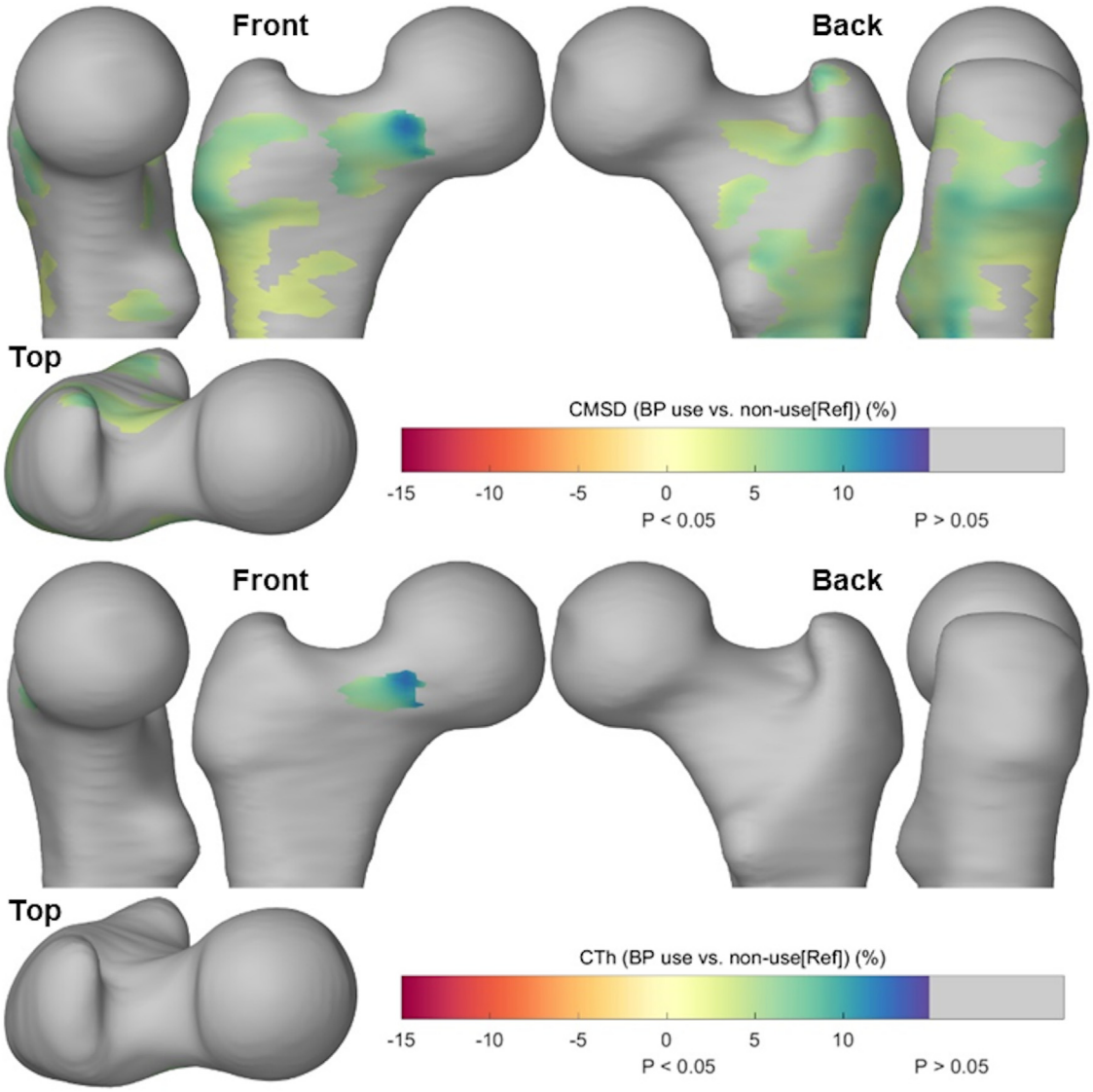

Fig. 2. 3D Cortical mapping of absolute difference in changes of cortical mass surface density (CMSD) and cortical thickness (CTh) in BP users vs. non-users during median 2 years in patients with early breast cancer on aromatase inhibitor treatment. Colored areas indicate key locations with significant difference in CMSD and CTh changes between BP users and non-users. BP use had a favorable effect on CMSD at the superior femoral neck and greater trochanter, with prominent changes in CTh at the superior femoral neck.

Table 3
Effect of bisphosphonate use on bone mineral density and cortical bone parameters in aromatase inhibitor users.

Sites	Adjusted beta coefficient (95% CI) (bisphosphonate user vs. non-user)*	P value
Percent change (%)		
Lumbar spine vBMD	+10.9 (+5.1 to + 16.8)	<0.001
Total hip CMSD	+3.7 (+1.8 to + 5.7)	<0.001
Total hip vBMD	+1.5 (-0.4 to + 3.3)	0.120
Femoral neck vBMD	+2.2 (+0.4 to + 4.1)	0.018
Femoral neck estimated cortical thickness (average)	+4.7 (+2.2 to + 7.1)	< 0.001
Quadrants		
Superior anterior, %	+12.8 (+3.1 to + 22.4)	0.010
Inferior anterior, %	+4.1 (+0.1 to + 8.2)	0.047
Inferior posterior, %	+3.1 (+0.4 to + 5.9)	0.025
Superior posterior, %	+8.0 (-4.1 to + 20.1)	0.193

*Adjusted for age, baseline femoral neck volumetric bone mineral density, and c-telopeptide level in multivariable linear regression models. Median follow-up duration was 757 days (interquartile range: 727–1109 days).Abbreviations: CMSD, cortical mass surface density.

a prior QCT-based study, older women had relatively preserved inferior femoral neck cortical bone across seven decades, whereas superior quadrants were most affected by cortical thinning and BMD loss during aging. [8] In line with this finding, in a prospective cohort of community-dwelling men and women, CTh at superior femoral neck best discriminated the risk of hip fracture independent of femoral neck aBMD among QCT-derived cortical parameters.[27] These findings suggest that cortical bone deficit, particularly at superior femoral neck, might be an important determinant of the resistance to hip fracture.

In a study conducted by Cheung et al., AIBL was associated with more dramatic changes in the cortical compartment than in the trabecular compartment in peripheral QCT scans of distal tibia and radius [28]. While the group treated with exemestane showed up to an eight-fold rapid decline in both CTh and area when compared to the placebo group, there was little difference in trabecular thickness or number between the two groups [28]. The authors argued that the effects of aromatase inhibitors on bone strength could not have been fully captured by central bone DXA testing

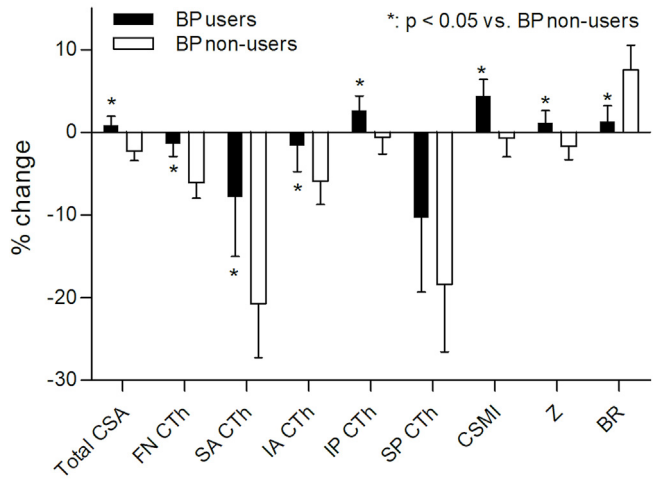

Fig. 3. Quadrant analysis of femoral neck cortex. BP users had a favorable profile in changes of cortical thickness and bone geometry parameters at the femoral neck. Abbreviations: CSA, cross-sectional area; FN, femoral neck; CTh, cortical thickness; SA, superior anterior; IA, inferior anterior; IP, inferior posterior; SP, superior posterior; CSMI, cross-sectional moment of inertia; Z, section modulus; BR, buckling ratio; BP, bisphosphonates.

[29]. In this study, we observed marked protection of cortical bone, particularly at superior femoral neck. It is conceivable that favorable effect of BP on cortical compartment of superior femoral neck observed in this study may confer additional fracture risk reduction in AIBL compared to the risk reduction predicted by changes in DXA aBMD; however, this needs to be validated in further studies.

Although our study primarily focused on changes in cortical bone, it should be noted that BP users showed clear gain in lumbar spine vBMD in patients with AIBL. Our finding supports previous studies that showed the robust improvement in DXA aBMD at lumbar spine. [23,30]

Our study has several limitations. Because this is a non-randomized observational study based on retrospective medical record review, BP users and non-users may have systemic differences, although we tried to match key baseline characteristics of the two groups as much as possible, with additional statistical adjustment in multivariable models. After propensity matching, the distribution of LSvBMD of BP users and non-users (77.2 vs. 80.7 mg/cm3) approximated to the reimbursement threshold of the health insurance review and assessment system of South Korea (<80 mg/cm^3), which indicated that clinical decision for initiating BP treatment was largely affected by health insurance reimbursement policy. In addition, clinicians' tendency to start bisphosphonate at earlier stage and fear of patients for the chronic complications of bisphosphonate could have affected the individual decisions to start bisphosphonate. The median 2-year follow-up duration might not be long enough to evaluate meaningful changes in bone structure. However, our study showed similar changes in BMD when compared to previous key randomized clinical trials with 24-month follow-up on BP treatment in postmenopausal women with early breast cancer [22,31]. Subgroup analyses based on the types of BPs were not possible due to limited sample size. Further studies on the effects of other antiresorptives, such as intravenous BP or denosumab, on cortical deficit in AIBL are needed. Although we used QCT scans reconstructed to 1-mm slice thickness to evaluate the cortical parameters of proximal femur, the resolution of clinical QCT data may not be sufficient to analyze intracortical remodeling and cortical porosity or to avoid the partial volume effect entirely [32]. However, the 3D CBM pipeline allowed us to perform a reliable, reproducible analysis of spatial heterogeneity in cortical parameters using clinical QCT [10-12].

In conclusion, BP use prevented cortical bone loss at key locations of the proximal femur in AIBL. BP use increased CMSD by up to 15% at key locations of the hip, such as the superior part of FN and greater trochanter. BP use prevented the thinning of average estimated CTh of FN, particularly at the superior anterior quadrant. Improvements in key locations of cortical femoral bone could support the effect of BP treatment in lowering the risk of hip fracture, which merits further investigation.

CRediT authorship contribution statement

Namki Hong: Conceptualization, Methodology, Data curation, Formal analysis, Investigation, Writing – original draft, Funding acquisition. **Seung Won Burm:** Data curation, Formal analysis, Investigation. **Graham Treece:** Methodology, Software, Writing – review & editing, Visualization, Validation. **Jee Ye Kim:** Writing – review & editing, Resources, Data curation. **Min Hwan Kim:** Writing – review & editing, Resources, Data curation. **Seunghyun Lee:** Writing – review & editing, Resources. **Sungjae Shin:** Writing – review & editing, Resources. **Yumie Rhee:** Resources, Supervision, Writing – review & editing, Project administration, Funding acquisition.

Declaration of Competing Interest

The authors declare that they have no known competing financial interests or personal relationships that could have appeared to influence the work reported in this paper.

Acknowledgement

We thank Keenan Brown (Mindways Software, Inc., TX, USA) for his insightful discussion and technical support.

Data availability

The data analyzed in this study are available upon reasonable request to the corresponding author (YR).

Funding

This work was supported by the Korea Medical Device Development Fund grant funded by the Korea government (the Ministry of Science and ICT, the Ministry of Trade, Industry and Energy, the Ministry of Health & Welfare, the Ministry of Food and Drug Safety, the National Research Foundation of Korea) (Project Number:1711139101, KMDF_PR_20210527_0003), the faculty research grant of Yonsei University College of Medicine, Seoul, Korea (6-2019-0102), and Korean Endocrine Society for New Faculty Convergence Research Award 2019. The funding sources or sponsors had no involvement throughout the study.

Ethical approval

This study was approved by the institutional review board of Severance Hospital, Seoul, Korea (IRB no. 4-2018-0635), with the requirement for informed consent waived due to the fact that medical records were reviewed in this study. All procedures performed in this study involving human participants were in accordance with the ethical standards of the institutional research committee and the 1964 Declaration of Helsinki and its later amendments.

Appendix A. Supplementary data

Supplementary data to this article can be found online at https://doi.org/10.1016/j.jbo.2021.100409.

References

[1] R.C. Coombes, L.S. Kilburn, C.F. Snowdon, R. Paridaens, R.E. Coleman, S.E. Jones, J. Jassem, C.J. Van de Velde, T. Delozier, I. Alvarez, L. Del Mastro, O. Ortmann, K. Diedrich, A.S. Coates, E. Bajetta, S.B. Holmberg, D. Dodwell, E. Mickiewicz, J. Andersen, P.E. Lønning, G. Cocconi, J. Forbes, M. Castiglione, N. Stuart, A. Stewart, L.J. Fallowfield, G. Bertelli, E. Hall, R.G. Bogle, M. Carpentieri, E. Colajori, M. Subar, E. Ireland, J.M. Bliss, Survival and safety of exemestane versus tamoxifen after 2–3 years' tamoxifen treatment (Intergroup Exemestane Study): a randomised controlled trial, Lancet 369 (9561) (2007) 559–570.

[2] B. Thürlimann, A. Keshaviah, A.S. Coates, H. Mouridsen, L. Mauriac, J.F. Forbes, R. Paridaens, M. Castiglione-Gertsch, R.D. Gelber, M. Rabaglio, I. Smith, A. Wardley, K.N. Price, A. Goldhirsch, A comparison of letrozole and tamoxifen in postmenopausal women with early breast cancer, N Engl J Med 353 (26) (2005) 2747–2757.

[3] P. Hadji, Aromatase inhibitor-associated bone loss in breast cancer patients is distinct from postmenopausal osteoporosis, Critical Reviews in Oncology/Hematology 69 (1) (2009) 73–82.

[4] S.J. Lee, K.M. Kim, J.K. Brown, A. Brett, Y.H. Roh, D.R. Kang, B.W. Park, Y. Rhee, Negative Impact of Aromatase Inhibitors on Proximal Femoral Bone Mass and Geometry in Postmenopausal Women with Breast Cancer, Calcif Tissue Int 97 (6) (2015) 551–559.

[5] M. Rabaglio, Z. Sun, K.N. Price, M. Castiglione-Gertsch, H. Hawle, B. Thürlimann, H. Mouridsen, M. Campone, J.F. Forbes, R.J. Paridaens, M. Colleoni, T. Pienkowski, J.-M. Nogaret, I. Láng, I. Smith, R.D. Gelber, A. Goldhirsch, A.S. Coates, Bone fractures among postmenopausal patients with endocrine-responsive early breast cancer treated with 5 years of letrozole or tamoxifen in the BIG 1–98 trial, Ann Oncol 20 (9) (2009) 1489–1498.

[6] F. Johannesdottir, E. Thrall, J. Muller, T.M. Keaveny, D.L. Kopperdahl, M.L. Bouxsein, Comparison of non-invasive assessments of strength of the proximal femur, Bone 105 (2017) 93–102.

[7] J. Reeve, N. Loveridge, The fragile elderly hip: Mechanisms associated with age-related loss of strength and toughness, Bone 61 (2014) 138–148.

[8] K.ES. Poole, P.M. Mayhew, C.M. Rose, J.K. Brown, P.J. Bearcroft, N. Loveridge, J. Reeve, Changing structure of the femoral neck across the adult female lifespan, J Bone Miner Res 25 (3) (2010) 482–491.

[9] P.M. Mayhew, C.D. Thomas, J.G. Clement, N. Loveridge, T.J. Beck, W. Bonfield, C. J. Burgoyne, J. Reeve, Relation between age, femoral neck cortical stability, and hip fracture risk, Lancet 366 (9480) (2005) 129–135.

[10] G.M. Treece, K.E. Poole, A.H. Gee, Imaging the femoral cortex: thickness, density and mass from clinical CT, Med Image Anal 16 (5) (2012) 952–965.

[11] G. Treece, A. Gee, Cortical Bone Mapping: Measurement and Statistical Analysis of Localised Skeletal Changes, Curr Osteoporos Rep 16 (5) (2018) 617–625.

[12] G.M. Treece, A.H. Gee, Independent measurement of femoral cortical thickness and cortical bone density using clinical CT, Med Image Anal 20 (1) (2015) 249–264.

[13] K.E.S. Poole, L. Skingle, A.H. Gee, T.D. Turmezei, F. Johannesdottir, K. Blesic, C. Rose, M. Vindlacheruvu, S. Donell, J. Vaculik, P. Dungl, M. Horak, J.J. Stepan, J. Reeve, G.M. Treece, Focal osteoporosis defects play a key role in hip fracture, Bone 94 (2017) 124–134.

[14] A. Yu, J. Carballido-Gamio, L. Wang, T.F. Lang, Y. Su, X. Wu, M. Wang, J. Wei, C. Yi, X. Cheng, Spatial Differences in the Distribution of Bone Between Femoral Neck and Trochanteric Fractures, Journal of bone and mineral research : the official journal of the American Society for Bone and Mineral Research 32 (8) (2017) 1672–1680.

[15] G.M. Treece, A.H. Gee, C. Tonkin, S.K. Ewing, P.M. Cawthon, D.M. Black, K.ES. Poole, Predicting Hip Fracture Type With Cortical Bone Mapping (CBM) in the Osteoporotic Fractures in Men (MrOS) Study, J Bone Miner Res 30 (11) (2015) 2067–2077.

[16] Adjuvant bisphosphonate treatment in early breast cancer: meta-analyses of individual patient data from randomised trials, The Lancet 386(10001) (2015) 1353-1361.

[17] C. Van Poznak, R.A. Hannon, J.R. Mackey, M. Campone, J.P. Apffelstaedt, G. Clack, D. Barlow, A. Makris, R. Eastell, Prevention of aromatase inhibitor-induced bone loss using risedronate: the SABRE trial, J Clin Oncol 28 (6) (2010) 967–975.

[18] C.E. Cann, J.E. Adams, J.K. Brown, A.D. Brett, H.A. Awad, CTXA hip–an extension of classical DXA measurements using quantitative CT, PloS one 9 (3) (2014) e91904.

[19] C.D. Thomas, P.M. Mayhew, J. Power, K.E. Poole, N. Loveridge, J.G. Clement, C.J. Burgoyne, J. Reeve, Femoral neck trabecular bone: loss with aging and role in preventing fracture, J Bone Miner Res 24 (11) (2009) 1808–1818.

[20] P.C. Austin, Optimal caliper widths for propensity-score matching when estimating differences in means and differences in proportions in observational studies, Pharmaceutical statistics 10 (2) (2011) 150–161.

[21] A.S. Elizabeth, Matching Methods for Causal Inference: A Review and a Look Forward, Statistical Science 25 (1) (2010) 1–21.

[22] S.L. Greenspan, K.T. Vujevich, A. Brufsky, B.C. Lembersky, G.J. van Londen, R.C. Jankowitz, S.L. Puhalla, P. Rastogi, S. Perera, Prevention of bone loss with risedronate in breast cancer survivors: a randomized, controlled clinical trial, Osteoporosis International 26 (6) (2015) 1857–1864.

[23] I. Sestak, S. Singh, J. Cuzick, G.M. Blake, R. Patel, F. Gossiel, R. Coleman, M. Dowsett, J.F. Forbes, A. Howell, R. Eastell, Changes in bone mineral density at 3 years in postmenopausal women receiving anastrozole and risedronate in the IBIS-II bone substudy: an international, double-blind, randomised, placebo-controlled trial, The Lancet Oncology 15 (13) (2014) 1460–1468.

[24] K. Waqas, J. Lima Ferreira, E. Tsourdi, J.J. Body, P. Hadji, M.C. Zillikens, Updated guidance on the management of cancer treatment-induced bone loss (CTIBL) in pre- and postmenopausal women with early-stage breast cancer, J Bone Oncol 28 (2021) 100355.

[25] J. Borggrefe, T. de Buhr, S. Shrestha, L.M. Marshall, E. Orwoll, K. Peters, D.M. Black, C.C. Glüer, Association of 3D Geometric Measures Derived From Quantitative Computed Tomography With Hip Fracture Risk in Older Men, J Bone Miner Res 31 (8) (2016) 1550–1558.

[26] L. Yang, W.J. Udall, E.V. McCloskey, R. Eastell, Distribution of bone density and cortical thickness in the proximal femur and their association with hip fracture in postmenopausal women: a quantitative computed tomography study, Osteoporos Int 25 (1) (2014) 251–263.

[27] F. Johannesdottir, K.E.S. Poole, J. Reeve, K. Siggeirsdottir, T. Aspelund, B. Mogensen, B.Y. Jonsson, S. Sigurdsson, T.B. Harris, V.G. Gudnason, G. Sigurdsson, Distribution of cortical bone in the femoral neck and hip fracture: a prospective case-control analysis of 143 incident hip fractures; the AGES-REYKJAVIK Study, Bone 48 (6) (2011) 1268–1276.

[28] A.M. Cheung, L. Tile, S. Cardew, S. Pruthi, J. Robbins, G. Tomlinson, M.K. Kapral, S. Khosla, S. Majumdar, M. Erlandson, J. Scher, H. Hu, A. Demaras, L. Lickley, L. Bordeleau, C. Elser, J. Ingle, H. Richardson, P.E. Goss, Bone density and structure in healthy postmenopausal women treated with exemestane for the primary prevention of breast cancer: a nested substudy of the MAP.3 randomised controlled trial, Lancet Oncol 13 (3) (2012) 275–284.

[29] J.A. Cauley, Bone loss associated with prevention of breast cancer, Lancet Oncol 13 (3) (2012) 221–222.

[30] P. Hadji, M.S. Aapro, J.J. Body, M. Gnant, M.L. Brandi, J.Y. Reginster, M.C. Zillikens, C.C. Glüer, T. de Villiers, R. Baber, G.D. Roodman, C. Cooper, B. Langdahl, S. Palacios, J. Kanis, N. Al-Daghri, X. Nogues, E.F. Eriksen, A. Kurth, R. Rizzoli, R.E. Coleman, Management of Aromatase Inhibitor-Associated Bone Loss (AIBL) in postmenopausal women with hormone sensitive breast cancer: Joint position statement of the IOF, CABS, ECTS, IEG, ESCEO IMS, and SIOG, Journal of bone oncology 7 (2017) 1–12.

[31] J.E. Lester, D. Dodwell, O.P. Purohit, S.A. Gutcher, S.P. Ellis, R. Thorpe, J.M. Horsman, J.E. Brown, R.A. Hannon, R.E. Coleman, Prevention of Anastrozole-Induced Bone Loss with Monthly Oral Ibandronate during Adjuvant Aromatase Inhibitor Therapy for Breast Cancer, Clinical Cancer Research 14 (19) (2008) 6336–6342.

[32] K.A. Davis, A.J. Burghardt, T.M. Link, S. Majumdar, The effects of geometric and threshold definitions on cortical bone metrics assessed by in vivo high-resolution peripheral quantitative computed tomography, Calcif Tissue Int 81 (5) (2007) 364–371.